Recognition of Distinctive Patterns of Gallium-67 Distribution in Sarcoidosis

Stephen B. Sulavik, Richard P. Spencer, David A. Weed, Howard R. Shapiro, Shyi-Tang Shiue, and Richard J. Castriotta

Pulmonary Division, Department of Medicine and Department of Nuclear Medicine, University of Connecticut School of Medicine, Farmington, Connecticut, and the Pulmonary Division, Department of Medicine and Department of Nuclear Medicine, Mount Sinai Hospital, Hartford, Connecticut

Assessment of gallium-67 (^{67}Ga) uptake in the salivary and lacrimal glands and intrathoracic lymph nodes was made in 605 consecutive patients including 65 with sarcoidosis. A distinctive intrathoracic lymph node ^{67}Ga uptake pattern, resembling the Greek letter lambda, was observed only in sarcoidosis (72%). Symmetrical lacrimal gland and parotid gland ^{67}Ga uptake (panda appearance) was noted in 79% of sarcoidosis patients. A simultaneous lambda and panda pattern (62%) or a panda appearance with radiographic bilateral, symmetrical, hilar lymphadenopathy (6%) was present only in sarcoidosis patients. The presence of either of these patterns was particularly prevalent in roentgen Stages I (80%) or II (74%). We conclude that simultaneous (a) lambda *and* panda images, or (b) a panda image *with* bilateral symmetrical hilar lymphadenopathy on chest X-ray represent distinctive patterns which are highly specific for sarcoidosis, and may obviate the need for invasive diagnostic procedures.

J Nucl Med 1990; 31:1909–1914

Bilateral symmetrical involvement of the salivary glands (*1–6*) and hilar lymph nodes (*7–10*) are well known characteristics and frequent features of sarcoidosis. Other conditions presently known to commonly affect the salivary glands *symmetrically* are few, i.e., viral parotitis, primary and secondary Sjögren's syndrome, and irradiation of the neck (*11*), and are not known to be associated with bilateral symmetrical hilar lymphadenopathy (BSHL) on chest X-ray.

Likewise, roentgen evidence of BSHL, as the main presenting clinical manifestation in diseases other than sarcoidosis is *exceedingly* rare (*9,10,12*), being observed in only a limited number of infections, namely, tuberculosis, fungal (histoplasmosis and coccidioidomycosis), and neoplastic, i.e., lymphoma and metastatic carcinoma (*12*), none of which are known to symmetrically involve the salivary glands. The simultaneous occurrence of bilateral symmetrical salivary gland *and* BSHL involvement may, therefore, represent an important diagnostic finding in strong support of the diagnosis of sarcoidosis. Both of these anatomic areas, when diseased, in most instances, are well visualized by ^{67}Ga imaging (*13–15*).

In preliminary reports (*16,17*), we assessed the prevalence of abnormal ^{67}Ga uptake of the head and thorax in sarcoidosis and other diseases. We found, as others have, a high prevalence in sarcoidosis of ^{67}Ga uptake in (a) the lacrimal (*18*) and salivary glands (*1,4,5*) (which when present in combination we have referred to as the panda appearance), and (b) of the hilar/mediastinal lymph nodes (*19–22*). However, with respect to the latter, we were impressed by the frequent finding of symmetrical, diffuse ^{67}Ga uptake, specifically of the parahilar, infrahilar, and right paratracheal or azygous (mediastinal) lymph nodes (which we have referred to as the lambda appearance) only in sarcoidosis patients. Although many others likely have seen this in sarcoidosis, this appears to be a new description, detailing specific location, extent, and pattern of hilar and mediastinal lymph node ^{67}Ga uptake in this disorder. Most significant from the viewpoint of diagnosis, was the observation found only in sarcoidosis patients of a *simultaneous* panda and lambda ^{67}Ga uptake image.

The purpose of the present study was to further evaluate the significance of these initial ^{67}Ga imaging observations as possible important aids in the noninvasive diagnosis of sarcoidosis.

PATIENTS AND METHODS

Gallium-67 imaging was performed 48 hr after the patient received an intravenous injection of 5 mCi of ^{67}Ga-citrate. Views were obtained with a large-field gamma scintillation camera with three photopeaks (93, 184, and 296 kV) each with a 20% window. The initial radiogallium image was for 600,000 counts. Other views were taken for the same time as indicated on the first view. Anterior, posterior, and lateral views of the head and thorax were obtained on all patients.

An analysis of ^{67}Ga images of the head (lacrimal and salivary glands) and thorax (intrathoracic lymph nodes) was

Received Feb. 14, 1990; revision accepted June 7, 1990.

For reprints contact: Stephen B. Sulavik, MD, Pulmonary Div., Dept. of Medicine, Rm. L-2080, Univ. of Connecticut Health Center, Farmington, CT 06032.

performed on 605 consecutive patients, referred to nuclear medicine for a wide variety of indications from January 1982 through October 1989. Analysis of lung ^{67}Ga uptake was not undertaken since lung involvement may be associated with virtually all of the disorders included in the differential diagnosis of sarcoidosis with frequent roentgen pattern overlap. Data were unavailable in 14 patients. All ^{67}Ga images were reviewed, and a consensus interpretation reached by at least two nuclear physicians and one pulmonary physician without knowledge of the name or diagnosis of any patient. All images were reviewed in the order in which they were obtained (consecutively) in the nuclear medicine department.

There were 65 patients with sarcoidosis and 540 patients with a variety of other disorders in this series. The diagnosis of sarcoidosis was made by organ biopsy in 54 patients and by a typical radiologic and clinical presentation in 11 patients, i.e., BSHL with or without bilateral, symmetrical lung infiltration (a) associated with erythema nodosum, acute uveal tract disease, 7th nerve palsy, and/or (b) supported by angiotensin converting enzyme elevation and/or significant broncho-alveolar lavage T-helper cell lymphocytosis (greater than 28%). All of these sarcoidosis patients have been followed for a minimum of 30 mo with a clinical course consistent with that of sarcoidosis. Only three sarcoidosis patients in this series were receiving corticosteroids at the time of radiogallium imaging.

The following Roentgen staging of sarcoidosis was used in this study: 0 = normal chest X-ray; I = BSHL, with or without right paratracheal (azygous) lymphadenopathy; II = BSHL *with* bilateral, symmetrical pulmonary infiltration; and III = bilateral symmetrical lung infiltration. All chest X-rays were reviewed by at least two radiologists and one pulmonary physician with a consensus opinion in all cases.

Lacrimal ^{67}Ga uptake and *abnormal* ^{67}Ga uptake of the salivary glands (parotid glands with or without submandibular glands) was considered to be present when the intensity of uptake, in the anterior projection, clearly exceeded that of the soft tissue and bone *between* the eyes or salivary glands and the nose; and in addition, revealed an unequivocal compact, well-defined visualization of ^{67}Ga uptake of these structures (Fig. 1). Although salivary gland ^{67}Ga uptake is often absent in normal individuals, in some normals ^{67}Ga uptake is greater than the adjacent soft tissues and bone (*5,23*). However, when this occurs, it appears as a diffuse and poorly demarcated ^{67}Ga uptake pattern (Fig. 1). Therefore, ^{67}Ga uptake in the salivary glands will be referred to only as normal or abnormal, since there is no apparent increased diagnostic value in using a radiogallium uptake grading scheme. Since ^{67}Ga uptake of the lacrimal glands is commonly observed in normal individuals, the qualifying terms "normal" or "abnormal" to describe ^{67}Ga lacrimal uptake will not be used.

It is important to distinguish salivary gland ^{67}Ga uptake versus cervical lymph node ^{67}Ga uptake, since the latter may rarely mimic the former on the anterior projection. The lateral projection helped to make this distinction. The presence and pattern of *parahilar* and *infrahilar* bronchopulmonary lymph node uptake, as well as mediastinal lymph node ^{67}Ga uptake, were carefully assessed, based upon their known anatomic distribution within the lung and mediastinum.

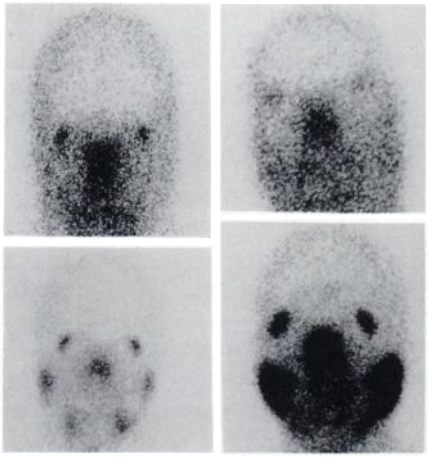

FIGURE 1
Upper panel (left): absent parotid gland ^{67}Ga uptake; (right): diffuse poorly demarcated ^{67}Ga uptake of parotids (normal variant). Lower panel: compact, discrete ^{67}Ga uptake of lacrimal and salivary glands (panda pattern).

RESULTS

Sarcoidosis Patients

The results of ^{67}Ga imaging in 65 patients with sarcoidosis according to Roentgen stages are summarized in Table 1.

Bilateral, symmetrical, ^{67}Ga uptake of the parahilar and infrahilar bronchopulmonary lymph node groups, associated with right paratracheal (azygous) lymph node ^{67}Ga uptake was a common finding in this series of sarcoidosis patients. This specific anatomic lymph node distribution correlated well with the known *normal* lymph node distribution of the parahilar and infrahilar bronchopulmonary and mediastinal lymph node groups in man (Fig. 2) (*24,25*), suggesting a *uniformly* distributed diffuse granulomatous involvement of these lymph nodes in sarcoidosis. Since this radiogallium image closely resembles the Greek letter lambda (λ), it was referred to as the "lambda" pattern, image, or

TABLE 1
Prevalence and Diagnostic Sensitivity of Distinctive Radiographic and/or ^{67}Ga Findings in 65 Sarcoidosis Patients According to Roentgen Stage

Roentgen stage	n	Lambda only	Panda only	Panda lambda	Diagnostic sensitivity*
0	9	1 (11%)	3 (30%)	5 (55%)	55%
I	25	2 (8%)	3 (12%)	17 (68%)	80%
II†	23	4 (17%)	1 (4%)	16 (70%)	74%
III‡	8	0 (0%)	4 (50%)	2 (25%)	25%
Total	65	7 (11%)	11 (17%)	40 (62%)	68%

n = number of patients.
* Presence of any one of the two distinctive radiographic and/or ^{67}Ga uptake patterns.
† Two patients had ^{67}Ga uptake of the lacrimal glands and lung only.
‡ One patient each had ^{67}Ga lacrimal gland uptake or parotid uptake only.

FIGURE 2
Upper panel: adaptation of the intrathoracic lymph node distribution in normal humans as described by Sukiennikow (*24*). Lower panel: Intrathoracic, mediastinal, and bronchopulmonary lymph node ^{67}Ga uptake in sarcoidosis (lambda pattern). Arrows in both panels: Upper: right paratracheal or azygous lymph node group (mediastinal); Lower: right and left para- and infrahilar lymph node groups (intrapulmonary); and Center: subcarinal lymph node group (mediastinal).

appearance (Fig. 3) (*17*) and was observed in 47 of 65 (72%) patients in this study. Significantly, a lambda pattern was present in 6 of 9 patients with normal chest X-rays (Stage 0). The lambda pattern was the *only* pattern of ^{67}Ga uptake of the intrathoracic lymph nodes observed in sarcoidosis patients.

Abnormal symmetrical ^{67}Ga uptake of the salivary glands and symmetrical ^{67}Ga uptake of the lacrimal glands were observed in 51 of 65 (79%) sarcoidosis patients. We refer to this specific ^{67}Ga image as the "panda" pattern, appearance, or image because of its resemblance to the face of a panda bear (Fig. 1) (*16, 17*). A panda pattern was present in 37 of 48 (77%) sarcoidosis patients with BSHL on chest X-ray (Stages I and II). Four patients demonstrated a panda pattern

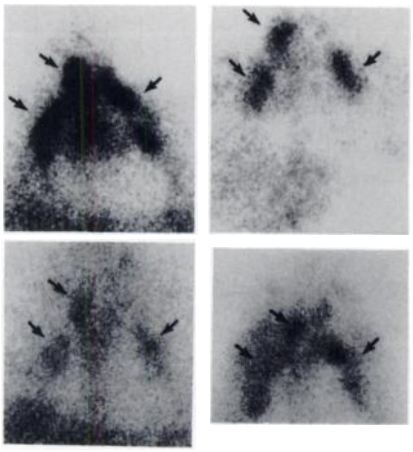

FIGURE 3
Sarcoidosis: lambda patterns of ^{67}Ga uptake. Arrows indicate right paratracheal (azygous) and para- and infrahilar lymph node uptake.

associated with BSHL only. A panda image was also observed in 8 of 9 (89%) patients with normal chest X-rays.

The *combination* of a lambda and a panda image was noted in 40 of 65 patients (62%) and in 33 of 48 patients (69%) who had associated BSHL (Stages I and II). This combination was also present in 5 of 8 (63%) sarcoidosis patients with normal chest X-rays.

A lambda, panda, or combination of the two was noted in 58 of 65 patients (89%). The remaining seven patients had abnormal ^{67}Ga distributions as follows: two patients had lacrimal and lung uptake only. Another two patients had increased lacrimal uptake only, and one patient had abnormal parotid gland uptake only. There was only one patient (Stage III) in this series who did not have ^{67}Ga lacrimal uptake.

Non-Sarcoidosis Patients

The diagnosis and results of ^{67}Ga imaging in 540 non-sarcoidosis patients are summarized in Tables 2 and 3. Table 2 summarizes those disorders associated with a panda or intrathoracic lymph node ^{67}Ga uptake. Table 3 summarizes the disorders associated with a normal ^{67}Ga scan of the head and thorax.

A panda pattern was observed in 23 non-sarcoidosis patients (4%). Radiographic symmetrical BSHL was not observed in any non-sarcoidosis "panda" patient. Excluding six patients who underwent irradiation to the neck, few disorders were associated with a panda image, i.e., 1° Sjögren's syndrome, collagen vascular

TABLE 2
Non-Sarcoid Disorders Associated with a Panda, Lambda, or Other Hilar/Mediastinal ^{67}Ga Image

Diagnosis	n	Lambda	Panda	H/M*
1° Sjögren's syndrome	16	0	8	0
Collagen disease				
SLE	20	0	2	0
RA	4	0	2	0
PSS	6‡	0	0	0
Lymphoma				
Hodgkin's (thoracic)				
Irradiated†	10	0	5	2
Nonirradiated	10	0	0	9
Hodgkin's (non-thoracic)	5‡	0	0	0
Non-Hodgkin's (thoracic)	7	0	0	7
(non-thoracic)	18‡	0	0	0
Leukemia	18	0	1§	0
Carcinoma	37	0	1†	5§
AIDS	14	0	2	0
EGL	1	0	1	0
Renal disease	29	0	1	0
Total	195	0	23	23

* Hilar/mediastinal.
† Irradiation of the neck.
‡ Listed in this table for clarity as a subset of the general disorder.
§ Myeloma, bladder (2), breast, and lung.

TABLE 3
Non-Sarcoid Disorders in Which a Lambda, Panda, or other Hilar/Mediastinal ^{67}Ga Uptake Pattern Was Absent

Diagnosis	n
Osteomyelitis	97
Non-pulmonary abscess	86
FUO	89
Miscellaneous	41
Non-malignant pulmonary disease	32
Total	345

n = number of patients.

diseases, acquired immunodeficiency syndrome (AIDS), acute lymphocytic leukemia (ALL) receiving chemotherapy, eosinophilic granuloma of lung (EGL), and renal failure.

A lambda pattern was not observed in any of 540 nonsarcoidosis patients. Hilar/mediastinal lymph node ^{67}Ga uptake, readily distinguishable from a lambda pattern, was observed in 23 patients (4%). These varied ^{67}Ga uptake patterns were *nonuniform*, *asymmetric*, and "bulky" in appearance (Fig. 4), unlike the *uniform* and *symmetrical* ^{67}Ga image observed in sarcoidosis patients, and were only noted in lymphoma (18 of 50 patients) and metastatic carcinoma (5 of 37 patients).

Statistical Analysis

Chi-square analysis was used to evaluate the statistical significance of the following groups of patients: those with (a) a panda *and* lambda ^{67}Ga uptake image, (b) a panda ^{67}Ga uptake image with BSHL on chest X-ray, and (c) a lambda ^{67}Ga uptake image only. The results of this analysis revealed $p < 0.0001$. These results are highly significant indicating that any of the above are excellent predictors of sarcoidosis.

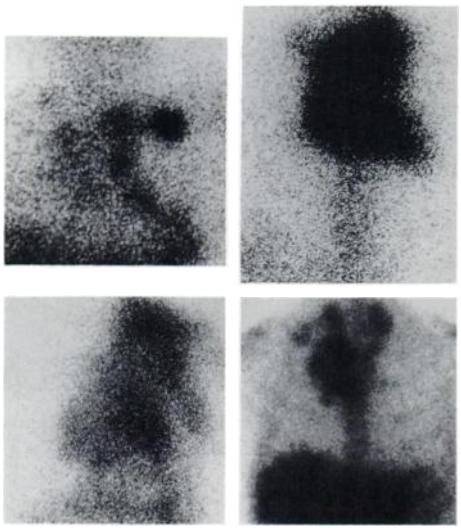

FIGURE 4
Intrathoracic lymph node ^{67}Ga uptake patterns in lymphoma (upper right and lower panels) and metastatic carcinoma (left upper panel).

DISCUSSION

The identification and high prevalence of a lambda pattern of symmetrical and uniform intrathoracic lymph node ^{67}Ga uptake (72%) and its frequent association with a panda pattern of lacrimal and abnormal salivary gland ^{67}Ga uptake (62%), *only* in sarcoidosis patients, were important findings in this study. These observations are also supported by several reports which have noted the high prevalence and potential diagnostic significance of the association of ^{67}Ga uptake in the lacrimal and/or salivary glands with lung and/or "hilar/mediastinal" lymph nodes (*1,5,18,19,22,26–29*). However, there is no previous mention of any *specific* pattern, i.e., a lambda appearance of ^{67}Ga uptake or its combination with a panda ^{67}Ga uptake image in sarcoidosis. Equally important was the finding of a panda pattern of ^{67}Ga uptake (in the absence of a ^{67}Ga lambda uptake pattern), associated with BSHL on chest X-ray only in sarcoidosis patients. The finding of one of these two combinations was observed in 80% of Stage I and 74% of Stage II sarcoidosis patients. Significantly, from the standpoint of initial diagnostic sensitivity, it is at these stages when the majority of patients (85%–90%) are first evaluated for a presumptive diagnosis of sarcoidosis and diagnostic procedures initiated.

A lambda pattern alone (11%) was also highly diagnostic of sarcoidosis in this study. Although extremely rare, the previously mentioned infectious and neoplastic diseases may present radiographically as BSHL only, on chest X-ray, mimicking Stage I sarcoidosis. This may be particularly important in adult HIV+ individuals who appear to have an increased prevalence of radiographic hilar/mediastinal lymph node involvement in mycobacterial (typical and atypical) as well as endemic fungal diseases. In these instances, it is possible, though as yet not observed, that a lambda ^{67}Ga pattern *alone* may be present. For these reasons, a lambda ^{67}Ga uptake pattern alone, although highly suggestive of sarcoidosis, cannot be considered to be specific for this disease.

The presence of a lambda *and* panda pattern in five of nine sarcoidosis patients in Stage 0 emphasizes the value of ^{67}Ga imaging of the head and thorax in suspected sarcoidosis, even in the absence of BSHL or lung infiltration on chest X-ray. "Hilar" uptake of ^{67}Ga in the absence of BSHL on chest X-ray in sarcoidosis has also been emphasized by Heshiki et al. (*19*). The *presenting* clinical manifestations in four of our five patients with Roentgen Stage 0 and typical ^{67}Ga pattern was somewhat unusual and included aseptic meningitis with bilateral uveitis, hepatosplenomegaly, hypercalcemia, and fever of unknown origin.

A panda pattern of abnormal symmetrical salivary

gland as well as lacrimal gland (usually intense) ^{67}Ga uptake was observed in 51 of 65 sarcoidosis patients (79%). Although a panda appearance without a lambda image or BSHL on chest X-ray was highly suggestive of sarcoidosis, this pattern alone was present in a significant percentage of patients with irradiation of the neck, primary Sjögren's syndrome, and in patients with AIDS. Irradiation of the neck, particularly in the treatment of Hodgkin's disease, is a well known cause (probably related to radiation induced sialoadenitis) of symmetric ^{67}Ga uptake of the salivary glands (*11*). Five of ten patients with neck irradiation for Hodgkin's lymphoma in this series demonstrated symmetric ^{67}Ga uptake of both the parotid and lacrimal glands. Symmetric ^{67}Ga uptake of the parotid glands has also been previously reported in Sjögren's syndrome (*30,31*). Eight of sixteen patients with primary Sjögren's syndrome in this study demonstrated symmetric ^{67}Ga uptake of both parotid and lacrimal glands. One patient with primary Sjögren's syndrome with parotid gland ^{67}Ga uptake, however, had no appreciable ^{67}Ga uptake of the lacrimal glands. As regards Sjögren's syndrome, symmetrical enlargement of the parotid glands and/or sicca syndrome (dryness of the eyes and mouth) may be due to sarcoidosis; also, Sjögren's syndrome may rarely precede the onset of overt lymphoma. The two patients demonstrating a panda appearance with AIDS may possibly represent a subclinical manifestation of the recently reported CD8 lymphocytosis syndrome associated with HIV+ serology (*32*). The possibility also exists that cytomegalovirus, which appears to have a predilection for the salivary glands, may be responsible. In those patients with systemic lupus erythematosis and peripheral rheumatoid arthritis with a panda image, it is tempting to speculate that subclinical "secondary" Sjögren's disease may be present. Salivary gland biopsy with ^{67}Ga uptake correlations will be necessary to establish possible causal relationships in these latter disorders. The significance of a panda image in one patient each with leukemia, EGL, and renal failure is not known. Other disorders in which a panda pattern has been observed include graft versus host disease (*33*) and CD8 lymphocytosis syndrome associated with HIV infection (*32*). A panda image by itself, therefore, is not specific for sarcoidosis, but may, however, strongly support or suggest only a limited number of readily diagnosable conditions.

In conclusion, a lambda in combination with a panda ^{67}Ga uptake pattern or a panda ^{67}Ga uptake pattern alone, associated with BSHL on chest X-ray (Fig. 5), represent distinctive patterns, which are highly specific for the diagnosis of sarcoidosis, as a result of its unique characteristics of symmetry, and predilection for the salivary glands, lacrimal glands and the hilar and mediastinal lymph nodes. Continued investigation of the aforementioned patterns in larger numbers of patients, is required, particularly in patients with lymphoma, infectious diseases, and especially those with HIV+ serology. Should further retrospective and prospective studies verify our results, the need for invasive diagnostic procedures such as lung and/or mediastinal biopsy, in the majority of sarcoidosis patients, will be obviated.

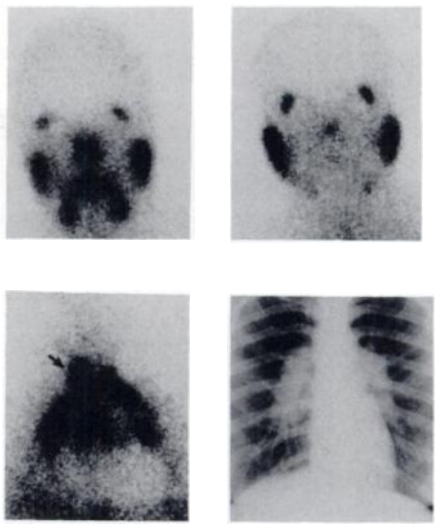

FIGURE 5
Sarcoidosis: Panda *and* lambda (left vertical panel); arrow indicates azygous lymph node group. Panda *and* BSHL (right vertical panel).

REFERENCES

1. Brantley SD, Orzel JA, Weiland FL, Bower JH. Parotid gland biopsy and ^{67}Ga imaging correlation in systemic sarcoidosis. *Chest* 1987; 91:403–407.
2. Dijkstra PF, Alberts C. Sialographic characteristics in sarcoidosis. *Eur J Respir Dis* 1984; 65:109–113.
3. Nessan VJ, Jacoway JR. Biopsy of minor salivary glands in the diagnosis of sarcoidosis. *N Engl J Med* 1979; 301:922–924.
4. Wiener SN, Patel BP. Ga-67-citrate uptake by the parotid glands in sarcoidosis. *Radiology* 1979; 130:753–755.
5. Mishkin FS, Tanaka TT, Niden AH. Abnormal gallium scan patterns of the salivary gland in pulmonary sarcoidosis. *Ann Intern Med* 1978; 89:933–935.
6. Bhoola KD, McNicol MW, Oliver S, Foran J. Changes in salivary enzymes in patients with sarcoidosis. *N Engl J Med* 1969; 281:877–879.
7. Lofgren S. Primary pulmonary sarcoidosis. I. Early signs and symptoms. *Acta Med Scand* 1953; 145:424–431.
8. Mayock RL, Bertrand R, Morrison CE, Scott JH, et al. Manifestations of sarcoidosis. *Am J Med* 1963; 35:67–89.
9. Winterbauer RH, Belie N, Moores KD. A clinical interpretation of bilateral hilar adenopathy. *Ann Intern Med* 1973; 78:65–71.
10. Sicherman HJ, Andersen HA, DeRemee RA. Sarcoidosis or fungal disease. *Chest* 1973; 64:36–37.
11. Bekerman C, Hoffer PB. Salivary gland uptake of ^{67}Ga-citrate following radiation therapy. *J Nucl Med* 1976; 17:685–687.
12. Scadding JG, Mitchell DN. In: *Sarcoidosis*. London: Chapman and Hall Ltd. Publ.; 1985:80.
13. Edwards CL, Hayes RL. Tumour scanning with ^{67}Ga-gallium citrate. *J Nucl Med* 1969; 10:103–105.

14. Nelson B, Hayes RL, Edwards CL, Knisely RM, Andrews GA. Distribution of gallium in human tissues after intravenous administration. *J Nucl Med* 1972; 13:92–100.
15. Higasi T, Nakayama Y, Murata A, et al. Clinical evaluation of ^{67}Ga-citrate scanning. *J Nucl Med* 1972; 13:196–201.
16. Sulavik SB, Weed D, Spencer R, Shapiro H, Castriotta R. A combinatorial analysis of ^{67}Ga scanning of the head and thorax in the diagnosis of sarcoidosis—the panda sign. In: C. Grassi, G. Rizzato, E. Pozzi, eds. *Sarcoidosis and other granulomatous disorders.* New York: Elsevier Science Publishers B.V.; 1988:517–518.
17. Sulavik SB, Weed D, Spencer R, Shapiro H, Shiue ST, Castriotta R. Gallium-67 imaging in the noninvasive diagnosis of sarcoidosis. *Sarcoidosis.* 6(suppl 1) 1989:115.
18. Karma A, Poukkula AA, Roukonen AO. Assessment of activity of ocular sarcoidosis by gallium scanning. *Br J Ophthalmol* 1987; 71:361–367.
19. Heshiki A, Sanford L, Schatz SL, et al. Gallium-67-citrate scanning in patients with pulmonary sarcoidosis. *Am J Roentgen* 1974; 122:744–749.
20. Israel HL, Park CH, Mansfield CM. Gallium scanning in sarcoidosis. *Ann NY Acad Sci* 1976; 278:514–516.
21. Israel HL, Gushue GF, Park CH. Assessment of gallium-67 scanning in pulmonary and extrapulmonary sarcoidosis. *Ann NY Acad Sci* 1986; 465:455–462.
22. Rohatgi PK. Significance of serum angiotensin converting enzyme and gallium scan in noninvasive diagnosis of sarcoidosis. *Eur J Respir Dis* 1980; 62:223–230.
23. Larson SM, Milder MS, Johnston GS. Interpretation of the ^{67}Ga photoscan. *J Nucl Med* 1972; 14:108–114.
24. Miller WS. *The Lung*, 2nd edition. Springfield, IL: Charles C. Thomas Publ.; 1947:121.
25. Sukiennikow W. *Topographische anatomie per bronchialen und trachealen lymphdrusen.* Berlin: 1903.
26. James DG. Ocular sarcoidosis. *Am J Med* 1959; 26:331–339.
27. Bekerman C, Szidon JP, Pinski S. The role of gallium-67 in the clinical evaluation of sarcoidosis. *Semin Roentgenol* 1985; 20(4):400–409.
28. Lauver JW, Gooneratne NS. Lacrimal, parotid and mediastinal uptake of gallium-67 in sarcoidosis. *Br J Radiol* 1979; 52:582–584.
29. Kohn H, Klech H, Mostbeck A, Kummer F. Ga-67 scanning for assessment of disease activity and therapy decisions in pulmonary sarcoidosis in comparison to chest radiography, serum ACE and blood T-lymphocytes. *Eur J Nucl Med* 1982; 7:413–416.
30. Logic JR, Ball GB, Tauze WN. Uptake of gallium-67 in parotid glands of patients with Sjögren's syndrome [Abstract]. *J Nucl Med* 1976; 17:530.
31. Collins RD, Ball GV, Logic JR. Gallium-67 scanning in Sjögren's syndrome: concise communication. *J Nucl Med* 1984; 25:299–302.
32. Itescu S, Brancato LJ, Buxbaum J, et al. A diffuse infiltrative CD8 lymphocytosis syndrome in human immunodeficiency virus (HIV) infection: a host immune response associated with HLA-DR5. *Ann Intern Med* 1990; 112(1):3–10.
33. Yamauchi K, Noguchi K, Suzuki Y, Nagao T. Gallium-67 uptake in the salivary glands in chronic graft-versus-host disease after bone marrow transplantation. *Clin Nucl Med* 1989; 14:330–332.